

Basic System Concept for Integrating a 2D and a 3D Radar and Designs of Automatic Detection Systems

G. V. TRUNK, B. H. CANTRELL, AND D. F. QUEEN

Radar Division

March 7, 1974



NAVAL RESEARCH LABORATORY
Washington, D.C.

REPORT DOCUMENTATION PAGE		READ INSTRUCTIONS BEFORE COMPLETING FORM
1. REPORT NUMBER NRL Report 7678	2. GOVT ACCESSION NO.	3. RECIPIENT'S CATALOG NUMBER
4. TITLE (and Subtitle) BASIC SYSTEM CONCEPT FOR INTEGRATING A 2D AND A 3D RADAR AND DESIGNS OF AUTOMATIC DETEC- TION SYSTEMS	5. TYPE OF REPORT & PERIOD COVERED Interim	
	6. PERFORMING ORG. REPORT NUMBER	
7. AUTHOR(s) Gerard V. Trunk, Ben H. Cantrell, and Donald F. Queen	8. CONTRACT OR GRANT NUMBER(s)	
9. PERFORMING ORGANIZATION NAME AND ADDRESS Naval Research Laboratory Washington, D.C. 20375	10. PROGRAM ELEMENT, PROJECT, TASK AREA & WORK UNIT NUMBERS NRL Problem R02-54 and R12-02 RF 12-151-403-4010 SF 12-141-703-17681	
11. CONTROLLING OFFICE NAME AND ADDRESS Department of the Navy Office of Naval Research Arlington, Va. 22217	12. REPORT DATE March 7, 1974	
	13. NUMBER OF PAGES 32	
14. MONITORING AGENCY NAME & ADDRESS (if different from Controlling Office)	15. SECURITY CLASS. (of this report) UNCLASSIFIED	
	15a. DECLASSIFICATION/DOWNGRADING SCHEDULE	
16. DISTRIBUTION STATEMENT (of this Report) Approved for public release; distribution unlimited.		
17. DISTRIBUTION STATEMENT (of the abstract entered in Block 20, if different from Report)		
18. SUPPLEMENTARY NOTES		
19. KEY WORDS (Continue on reverse side if necessary and identify by block number) Sensor integration Detectors Nonparametric detectors Radar		
20. ABSTRACT (Continue on reverse side if necessary and identify by block number) A basic system concept of digitally integrating any 2D radar and any frequency-scan 3D radar was applied to the SPS-12 and SPS-39 radars, giving a composite coverage with nulls greatly decreased from those of the SPS-12 pattern. Both radars operate in a search mode, automatic detection systems are associated with each radar, and the detection information is integrated via the tracking system. Height information is provided on targets designated by either the radar operator or the tracking computer.		

(Continued)

Three automatic detectors, a generalized sign nonparametric processor with adaptive thresholding, a rank detector, and a log-Rayleigh detector, were designed. Using Monte Carlo techniques, probability of detection curves and angular accuracy curves were generated for these detectors. An unexpected result was little difference between the log-Rayleigh and rank detectors.

CONTENTS

INTRODUCTION	1
SPS-12 AND SPS-39 RADAR OPERATION	1
AUTOMATIC DETECTION	3
SPS-12 Radar	4
First Threshold	5
Integrator	5
Second Threshold	10
SPS-39 (lower Beam)	14
SPS-39 (Upper Beam)	17
Rank Detector	17
Log Rayleigh Detector	17
Comparison	20
SPS-39 (Scanning Beam)	21
AZIMUTHAL ESTIMATES	21
SUMMARY	24
REFERENCES	24
APPENDIX A—Monte Carlo Simulation	26
APPENDIX B—Importance Sampling	28

BASIC SYSTEM CONCEPT FOR INTEGRATING A 2D AND A 3D RADAR AND DESIGNS OF AUTOMATIC DETECTION SYSTEMS

INTRODUCTION

On board most naval combat vessels are two kinds of surveillance radars: 2D radars and 3D radars. To obtain the maximum information available, one should combine the information obtained with both radars. However in today's Navy there is neither communication between the radars nor correlation of the outputs of the radars. This report describes a portion of a project which is concerned with the *integration* of information obtained with various radars. Specifically the project is concerned with the digital integration of the 2D SPS-12 and the 3D SPS-39 radars. The methods used will not be restricted to these two radars but will be applicable to any 2D radar and any frequency-scan 3D radar.

The basic system concept is illustrated in Fig. 1. The SPS-12 and SPS-39 radars are used for surveillance. The SPS-12 operates in its normal mode, and the SPS-39 operates in a modified mode which will be described in the next section. Automatic target-detection (ATD) systems are associated with each radar. The ATD systems are the main subject of this report. These ATD systems not only detect targets but also estimate the target's azimuthal position and inhibit detections in neighboring range cells. The detections are then transmitted to the tracking computer. The computer accepts detections from both radars, integrates (combines) them into a single track file, and displays them. The radar operator interacts with the system via the display. Some of the operator functions are requests for information on various targets and demands for height on selected targets. When a height demand is received, the tracking computer calculates the next update time for the SPS-39 and at this time sends a message to the SPS-39 to stop its search pattern and perform an elevation scan pattern. The elevation of the selected target is then sent back to the tracking computer. In addition to height demands generated by the radar operator, height demands may also be generated by the tracking computer.

The system will be used to evaluate not only the benefits of sensor integration but also the ability to hand off designated targets from the track file to a tracking radar. Of special interest is the ability to hand off to a tracking radar directly from a 2D track.

SPS-12 AND SPS-39 RADAR OPERATION

The SPS-12 is a typical L-band search radar, and some of its fundamental parameters are shown in Table 1. At a rotation rate of 7.5 rpm, 30 hits are obtained on the target; and at a rotation of 15 rpm, 15 hits are obtained on the target. The coverage pattern for the SPS-12 located 166 feet above water (on top of building 75 at the Chesapeake Bay Division of NRL) was calculated using Blake's computer program [1], and the result is

Manuscript submitted October 24, 1973.

TRUNK, CANTRELL AND QUEEN

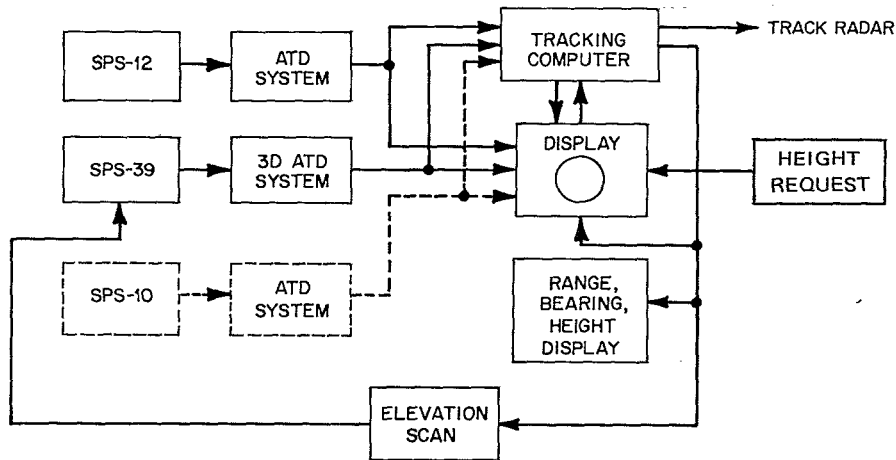


Fig. 1—Basic system concept for sensor integration

Table 1
Some SPS-12 Radar Parameters

Parameter	Value
Frequency (MHz)	1250-1350
Pulse length (μ s)	1, (4)
Pulse rate (pps)	600, (300)
Ave. power (watts)	600
Noise figure (dB)	9
Polarization	Horizontal
Hor. beamwidth (deg)	3.3
Ver. beamwidth (deg)	30
Scan rate (rpm)	2.5-15

shown in Fig. 2. The familiar lobing pattern due to multipath is present. If one tried to perform automatic tracking with this radar or any other naval 2D radar, one would encounter severe fading conditions which make it difficult to maintain tracks [2].

To reduce the fading problem, two lower beams of the SPS-39 will be used to fill in the nulls of the SPS-12. (The normal search pattern of the SPS-39 will not be used.) Blake's computer program [1] was modified (by Joe Goldstein) to obtain the composite coverage pattern of several radars. If one transmits two beams with the SPS-39 and obtains eight hits with the beam pointed at 3.3° and 15 hits with the beam pointed at 1.8° , one obtains the composite coverage pattern of the two radars that is shown in Fig. 3. Comparing Figs. 2 and 3, one should note that between 1° and 5° very few nulls exist in the composite pattern and that below 1° the nulls are narrower and not as deep for the composite pattern.

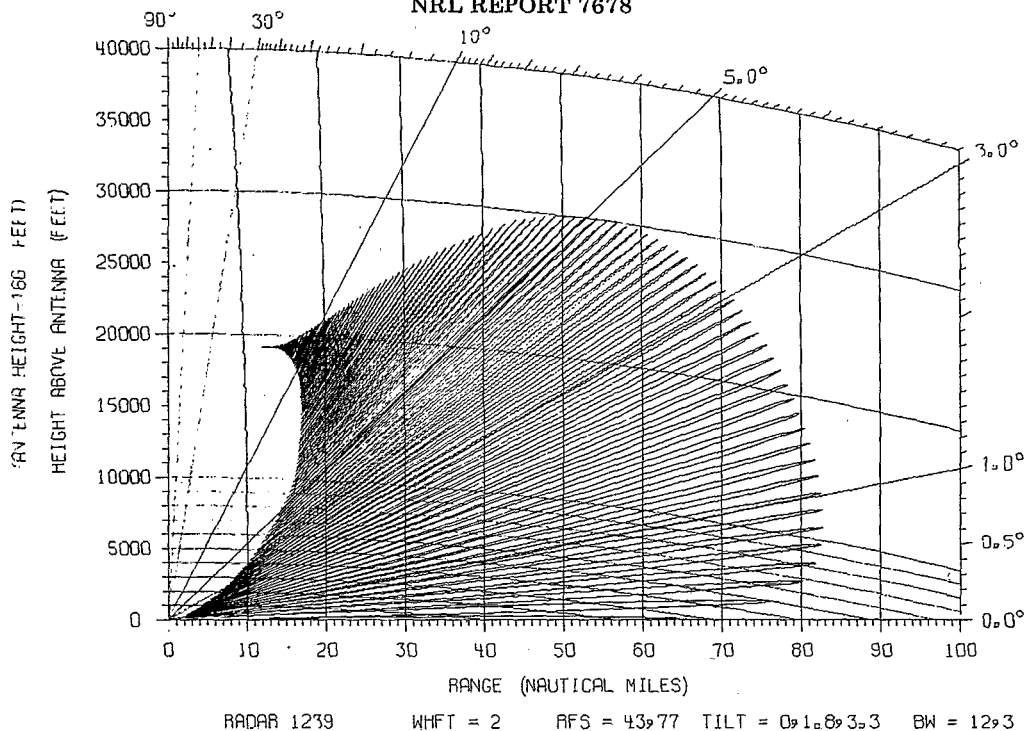


Fig. 2—Antenna pattern for the SPS-12 radar, with an antenna height of 166 feet and a free-space range of 42.5 n.mi.

AUTOMATIC DETECTION

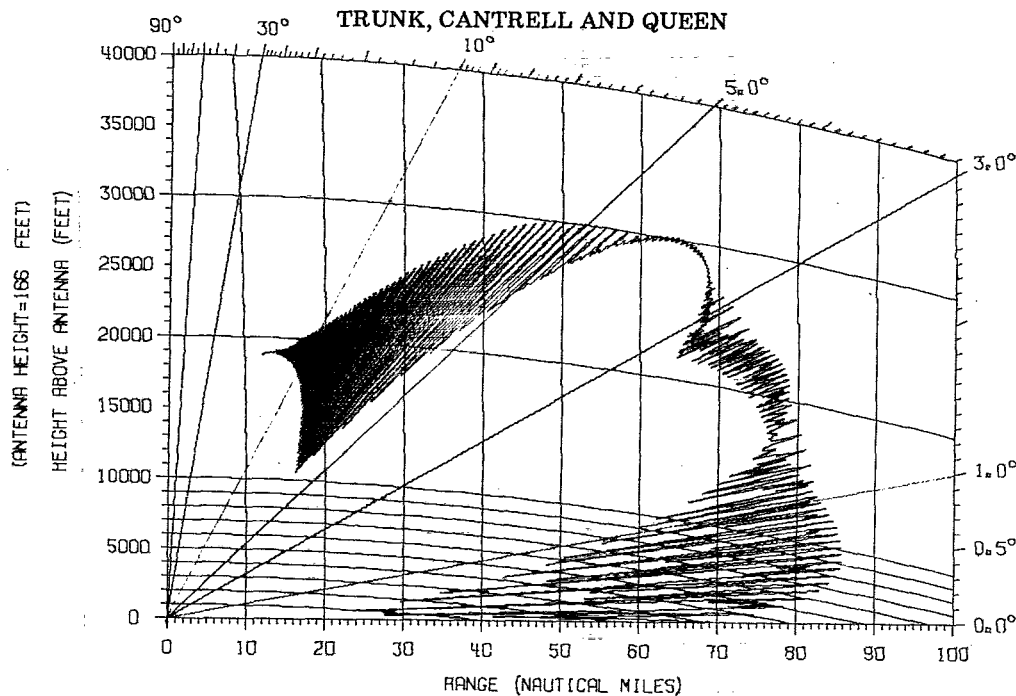
In the detection process, usually three operations are performed:

- Quantization of the data,
- Integration of the data,
- Thresholding of the data (decision process).

These operations are performed whether an operator is making a decision using a PPI or an automatic detection circuit is operating on the data. The main problem associated with ATD systems is how to perform these three operations while maintaining a constant false-alarm rate (CFAR) without losing target sensitivity.

In determining what kind of detector to use for CFAR, the most important parameter is the number of pulses on target. In 2D radars, where there are many pulses on the target, nonparametric detectors provide CFAR for unknown noise distributions and power levels. For 3D radars, where there are few pulses on target, adaptive thresholds provide CFAR for known noise distributions with unknown power levels.

The SPS-12 has from 15 to 30 pulses on target; consequently the nonparametric detector will be used. The SPS-39 is being used in a special mode. In the lower beam there are 15 pulses per beamwidth, and a nonparametric detector is used. In the upper beam there are only seven pulses per beamwidth, and whether a nonparametric detector or an adaptive threshold is best is still an open question.



RADAR 1239 WHFT = 2 RFS = 43.77 TILT = 0.1.8.3.3 BW = 12.3

Fig. 3—Composite antenna pattern for the SPS-12 and SPS-39 radars. The antenna height is 166 feet, the free-space range of the SPS-12 is 42.5 n.mi., the free-space range of the 1.8° elevation beam of the SPS-39 is 77 n.mi., and the free space range of the 3.3° elevation beam is 68.6 n.mi.

SPS-12 Radar

As mentioned, a nonparametric detector will be used with the SPS-12. Since the amount of literature about the various nonparametric detectors is enormous, no attempt will be made to review the subject. Rather, as a starting point, we will consider the generalized sign nonparametric processor with adaptive thresholding suggested by APL [3].

Let x_{ij} be the i th returned pulse in the j th range cell. The rank R_{ij} of the i th pulse in the j th cell is

$$R_{ij} = \sum_k u(x_{ij} - x_{ik}), \quad (1)$$

where

$$u(x) = 1, \quad x > 0,$$

$$u(x) = 0, \quad x \leq 0,$$

and the k summation is over the L range cells surrounding the j th cell. If there are M pulses within the beamwidth, the ranks are integrated (summed) as follows

$$Z_{ij} = \sum_{k=i+1-M}^i R_{kj}. \quad (2)$$

The detection decision is made by comparing Z_{ij} to an adaptive threshold $T_{ij}(Z_{ij})$ and noting the sign. The adaptive threshold is used to take into account the fact that the ranks of successive pulses can be correlated. This correlation is due to correlated clutter or receiver noise out of the MTI. This sign detector can be divided into three parts:

- A first threshold which ranks the data, namely, Eq. (1),
- An integrator, Eq. (2),
- A second threshold, which is the decision process.

First Threshold

The block diagram of the nonparametric rank detector, which is the first threshold, is shown in Fig. 4. The logarithmic detector is used because it has a larger dynamic range than the linear detector. The output of the logarithmic detector is then digitalized using an eight-bit A/D convertor. The last 18 eight-bit words are saved in shift registers. The center (test) sample is then compared to each of the first eight samples and last seven samples. If the center sample is greater than the sample, the output of the comparator is 1; if the center sample is less than the sample, the output is 0; and if the center sample is equal to the sample, the output is either 0 or 1 depending on whether the comparator is odd or even. The outputs of the comparators are summed to form the rank of the test sample. The samples on either side of the center cell are not used in the comparison, because when a target is present, the Gaussian pulse shape will cause target returns in the adjacent cells.

Integrator

There are two reasons the sum integrator, Eq. (2), will not be used:

- First, as the radar beam sweeps by the target, the returned signal is modulated by the antenna pattern. Consequently, to maximize the probability of detection, the ranks should be weighted as to reflect this changing signal-to-noise ratio (S/N).
- Second, the hardware requirements for the moving-window rank detector, Eq. (2), can be fairly large. If there are N_R range cells and M pulses per beamwidth, one

needs to store MN_R four-bit words. The storage requirements for the SPS-12 would be about 4×10^4 words.*

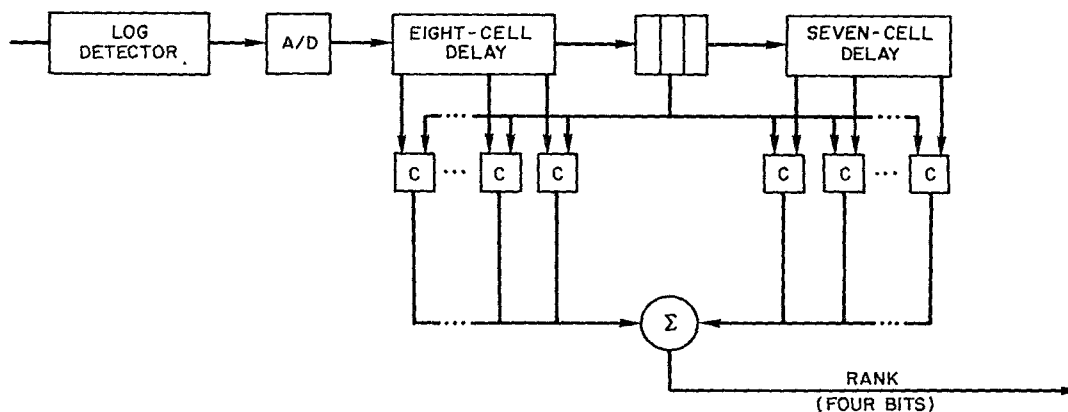


Fig. 4—Nonparametric rank detector, a first-threshold circuit

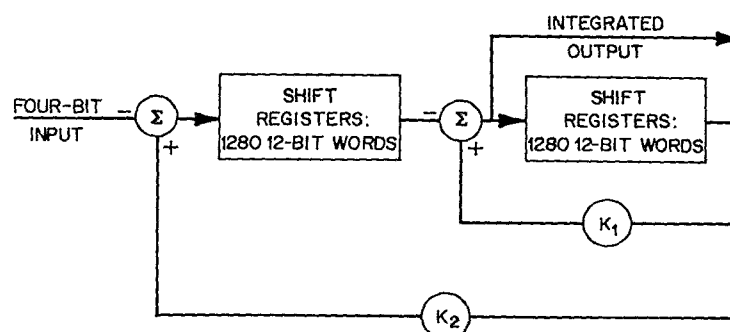


Fig. 5—A two-pole Integrator for ranked samples

The integrator that will be used is a two-pole filter (Fig. 5). As shown in Fig. 6, the weighting function of the two-pole filter is similar to the modulation function the scanning antenna applies to the returned signal. Since the two-pole filter [4] was designed for envelope detected signals, not ranked samples, the analysis will be sketched.

At a given range cell the output w_i of an envelope detector under both hypotheses, noise and signal-plus-noise, is

$$H_0: w_i = n_i,$$

$$H_1: w_i = n_i + A_i,$$

*Storage requirements for the UHF 2D radars would be about 10^5 words.

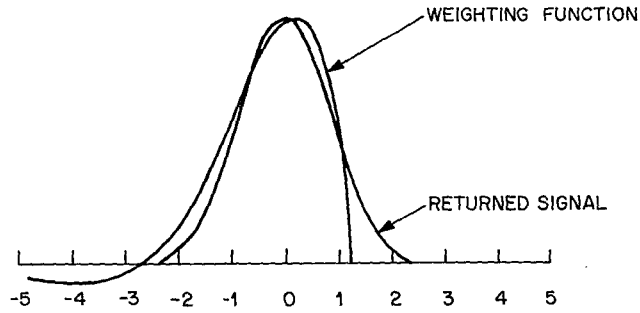


Fig. 6—Optimum weighting function of the two-pole filter shown in Fig. 5

where n_i is Rayleigh-distributed noise and A_i is the signal on the i th sweep of the radar. As seen from Fig. 4, if the noise in the neighboring range cells is identically distributed, the probability density of the rank R_i under H_0 is

$$p(R_i = \ell | H_0) = \frac{1}{16}, \quad \ell = 0, 1, \dots, 15. \quad (3)$$

Even though n_i has been assumed to be Rayleigh distributed, Eq. (3) is valid as long as the noise samples are only *identically distributed*. When the test cell contains signal and the reference cells contain noise, the probability density is [5]

$$p(R_i = \ell | H_1) = e^{(-S/N)_i} \binom{15}{\ell} \sum_{k=0}^{\ell} (-1)^k \binom{\ell}{k} \frac{1}{16 - \ell + k} e^{(S/N)_i / (16 - \ell + k)}, \quad \ell = 0, 1, \dots, 15, \quad (4)$$

where $(S/N)_i$ is S/N on the i th pulse and the noise is Rayleigh distributed. Now

$$(S/N)_i = (S/N)_c G^4(i), \quad (5)$$

where $(S/N)_c$ is S/N at the center of the beam and $G(i)$ is the voltage-gain antenna pattern on the i th pulse. In this report we assume

$$G^2(i) = \frac{\sin^2 (i\alpha\Delta\theta - \pi)}{(i\alpha\Delta\theta - \pi)^2}, \quad 0 \leq i \leq \frac{2\pi}{\alpha\Delta\theta}, \quad (6a)$$

$$= 0, \quad \text{otherwise,} \quad (6b)$$

where $\alpha = 1.3916\beta$, 2β is the 3-dB beamwidth, and $\Delta\theta$ is the angular increment of the scanning radar and equals $2\pi(t/T)$, with T being the scan time of the radar and t being the sampling time, which is the reciprocal of the pulse repetition rate.

The output of the two-pole integrator [4] is

$$Z(i) = \Phi Z(i-1) + \Gamma R_i, \quad (7)$$

where

$$\Phi = \begin{bmatrix} 0 & k_2 \\ -1 & k_1 \end{bmatrix},$$

$$Z(i) = \begin{bmatrix} Z_1(i) \\ Z_2(i) \end{bmatrix},$$

$$\Gamma = \begin{bmatrix} -1 \\ 0 \end{bmatrix}.$$

The integrator is optimized by adjusting the parameters k_1 and k_2 to maximize S/N at the output of the filter; specifically, one maximizes

$$\left(\frac{S}{N}\right)_0 = \frac{Z^2(i^*)}{\text{var}[Z_2(i)|H_0]}, \quad (8)$$

where i^* is the pulse at which the filter obtains its maximum value when excited with

$$R_i = E[R_i|H_1] - E[R_i|H_0].$$

Using

$$E[R_i|H_0] = 7.5,$$

$$E[R_i|H_1] = \sum_{\ell=0}^{15} \ell p(R_i = \ell|H_1),$$

$$\text{var}[R_i|H_0] = 21.25,$$

and

$$\text{var}[Z_2(i)|H_0] = \frac{\text{var}[R_i|H_0]}{1 - k_1^2 - k_2^2 + 2k_1^2k_2/(1 + k_2)}$$

the Hooke and Jeeves [6] direct search technique was used to maximize $(S/N)_0$. The coefficients for several cases are shown in Table 2.

Since the two-pole filter is implemented digitally, the coefficients should be inverse powers of 2; that is, $k = \sum a_j/2^j$, $a_j = 0$ or 1. This restriction was placed on the coefficients, $(S/N)_0$ was maximized again, and the results are shown in Table 3. Using these numbers, multiplication can be performed fast. For instance $1.111 \times B$ can be performed by subtracting B shifted three places to the right from B shifted one place to the left.

Table 2
Values of k_1 and k_2 to Maximize $(S/N)_0$ for Various Cases

No. of Pulses in Beamwidth	Optimum Values	
	k_1	k_2
30	1.8922	0.8991
15	1.7814	0.8073
7	1.5848	0.6715

Table 3
Binary Values of k_1 and k_2 to Maximize $(S/N)_0$ for the SPS-12 Radar

No. of Pulses in Beamwidth	Optimum Values	
	k_1	k_2
30	1.111	0.1110001
15	1.11	0.11001

The number of bits in the shift register is set by noting the maximum value under steady-state conditions. If the input is taken to be 15, the steady state values of the two shift registers are

$$Z_1(i) = \frac{(k_1 - 1)15}{1 + k_2 - k_1}, \tag{9}$$

$$Z_2(i) = \frac{15}{1 + k_2 - k_1}. \tag{10}$$

Using the values in Table 3, the steady-state values are 1680 and 1920 respectively for $Z_1(i)$ and $Z_2(i)$ for the case of 30 pulses on target. Thus 11 bits are required for storage. However we have decided to store also a roundoff bit and consequently are using 12 bits. Finally, the multiplications (series of additions and subtractions) are performed in 16 bits to reduce roundoff errors, and the shift registers are initialized to their mean values 840 and 960.

Second Threshold

Since the reference samples are not always independent and identically distributed, a fixed threshold cannot be used, because it would yield too many false alarms. Consequently an adaptive second threshold will be used. The threshold suggested by APL is shown in Fig. 7. This circuit works as follows: The reference cells are summed, and their average is found. The average is subtracted from every sample, and the absolute value A is taken. The absolute values are now summed to form the mean-deviation estimate of the standard deviation [3]:

$$\hat{\sigma} = \sqrt{\pi/[2N(N-1)]} \sum_{j=1}^N |Z_j - \bar{Z}|, \quad (11)$$

where

$$\bar{Z} = \sum_{j=1}^N Z_j \quad (12)$$

and the Z values are Gaussian distributed with variance σ^2 . The detection decision is made by subtracting \bar{Z} from the test cell, multiplying by the result by k , and comparing this to the sum of mean deviates. Consequently this detector is equivalent to comparing the test cell to an adaptive threshold T , where

$$\bar{Z} + \frac{\sqrt{\pi/[2N(N-1)]}}{k} \hat{\sigma}. \quad (13)$$

Since the density of Z values (sum of ranks) is approximated accurately by a Gaussian density, the adaptive threshold provides adequate CFAR action in correlated clutter [3]. However, there are two problems with this adaptive threshold:

- First, through the detector is conceptually simple, the implementation involves quite an amount of hardware and logic levels. To make a decision, one must go through ten logic levels (seven additions, a right shift, an absolute value, and a comparison). Thus for small pulse widths the timing will become critical.

- Second, and more important, target sensitivity is less when an extraneous target is in the reference cells. The extraneous target competes with the test cell for high ranks and causes the second threshold to be very high. To confirm this, a Monte Carlo simulation (described in Appendix A) was used to calculate the probability of detection versus

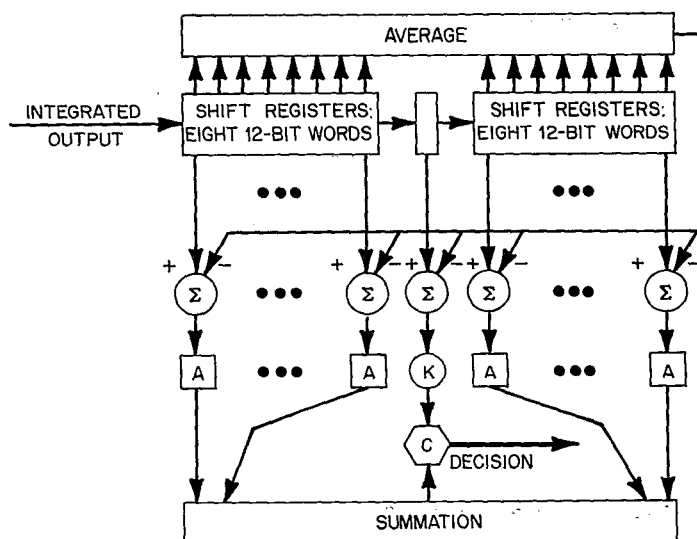


Fig. 7—Second-threshold device suggested by APL

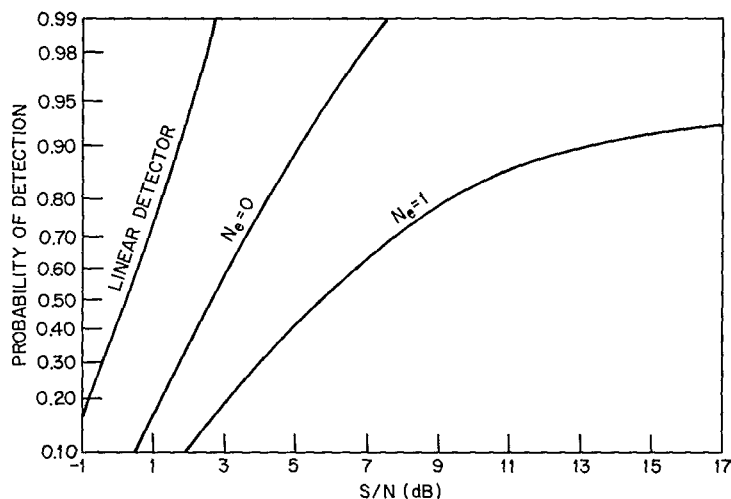


Fig. 8—Probability of detection versus S/N for the generalized sign test with adaptive thresholding which was suggested by APL ($M = 30$ pulses and $P_{fa} = 10^{-6}$). The linear-detector curve is shown for comparison. N_e is the number of extraneous targets (of the same strength as the target) in the reference cells

S/N , and the results are shown in Fig. 8. The curve marked linear detector is the linear-envelope-detector curve for 32 equal-amplitude pulses taken from Robertson [7]. Comparing the $N_e = 0$ and $N_e = 1$ curves at $P_D = 0.9$, one finds about an 8-dB loss due to the extraneous target. Comparing the $N_e = 0$ curve and the linear detection curve at $P_D = 0.9$ one finds a 3.3-dB difference. This 3.3-dB difference is due to the facts that the rank detector is a nonoptimum detector and the simulation includes the 1.6-dB “scanning loss” [8].

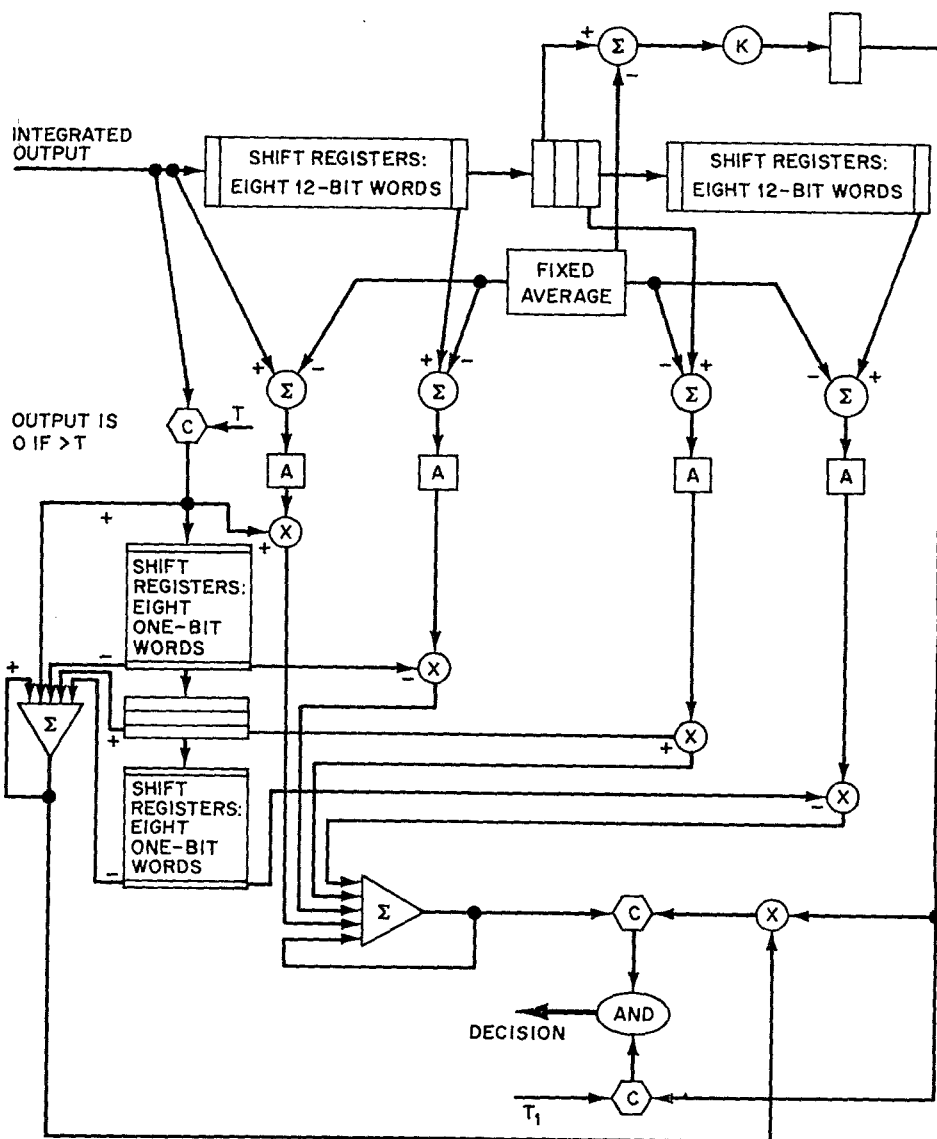


Fig. 9—Second-threshold device modified by NRL

To reduce the number of logic levels and the loss due to extraneous targets in the reference cells, a new second threshold has been designed. This threshold is shown in Fig. 9 and differs from APL's threshold in three ways:

- The mean value of the reference cells is *not* calculated. Instead the nonparametric mean value (960), which is equal to the mean rank (7.5) times the gain (128) of the two-pole filter, is used. It can be used because even though the ranks are correlated, the average rank is still 7.5.

• The extraneous targets are removed by a preliminary threshold T [9], which corresponds to $P_{fa} = 10^{-2}$. If the reference sample is greater than T , it is removed from the calculation of the standard deviation. However, if a sample is removed, the mean deviate is no longer an unbiased estimate of σ , since the fixed mean is not the mean of the reference sample when a high sample has been removed. Consequently, let us calculate $E|Z_i - F\mu|$ where μ is the mean of the Gaussian variable Z_i and F is a constant:

$$E|Z_i - F\mu| = \int_{-\infty}^{\infty} |Z - F\mu| \frac{1}{\sqrt{2\pi\sigma^2}} e^{-(Z-\mu)/2\sigma^2} dZ. \quad (14)$$

Letting $y = (x - \mu)/\sigma$, removing the absolute-value sign by breaking the integral into two integrals, and integrating, we obtain

$$E|Z_i - F\mu| = \frac{2\sigma}{\sqrt{2\pi}} e^{-(F-1)^2\mu^2/2\sigma^2} + (F-1)\mu \left\{ 2\Phi \left[\frac{(F-1)\mu}{\sigma} \right] - 1 \right\}, \quad (15)$$

where

$$\Phi(X) = \int_{-\infty}^X \frac{1}{\sqrt{2\pi}} e^{-y^2/2} dy. \quad (16)$$

If no reference cells are above the threshold T , $F = 1$ and $E|Z - 960| = 86.04$, since

$$\mu = \frac{\frac{L}{2}}{1 + k_2 - k_1}$$

and

$$\sigma^2 = \frac{\frac{1}{L+1} \sum_{\ell=0}^L \ell^2 - \left(\frac{1}{L+1} \sum_{\ell=0}^L \ell \right)^2}{1 - k_1^2 - k_2^2 + 2k_1^2 k_2 / (1 + k_2)},$$

where L is the number of noise reference cells used in the first threshold: $L = 15$. If one cell is above the threshold T and we assume that the extraneous target always obtains a rank of 15, any of the noise samples can take on a maximum value of only 14; that is, $L = 14$. Consequently $\mu = 896$, $F = 15/14$ ($960/896$), $\sigma = 101.07$, and $E|Z - 960| = 96.16$ from Eq. (15). Furthermore, if in addition to the extraneous target in the reference cell the test cell contains a strong target, the noise reference cell possibly could obtain a maximum value of only 13. Thus $L = 13$, $\mu = 832$, $F = 15/13$ ($960/832$), $\sigma = 94.30$, and

$E|Z - 960| = 135.54$. When there is a reference cell greater than the threshold T , if one wants to maintain the same P_{fa} , one should reduce the estimate of σ by 0.895 (86.04/96.16). However, if one wants to maintain the same target sensitivity, one should reduce the estimate of σ by 0.635 (86.04/135.54). As a compromise the estimate of σ will be reduced by a factor of 0.82. Because of hardware implementation problems, this factor will be used for zero or more than one reference cell above T . This can be done because of the following third change, which involves another fixed threshold.

- In addition to the test cell being above the adaptive threshold T , the test cell must be above a fixed threshold T_1 for a target to be declared. This threshold corresponds to $P_{fa} = 10^{-6}$ when the reference cells are independent and identically distributed. The threshold value T_1 for a given P_{fa} was found using the importance-sampling technique [10] which is described in Appendix B. The curve for $M = 30$ pulses is shown in Fig. 10.

At the beginning of operation the second threshold for $M = 30$ is initialized in the following manner: the average value is set to 960, and this value is stored in the 12-bit shift registers; zeros are stored in the one-bit shift registers, and their sum is set to zero; the running sum of the mean deviates is set to zero; and also set are $k = 0.205$,* $T = 1200$ ($P_{fa} = 10^{-2}$), and $T_1 = (1460 - 960)k = 102.5$.

The detection curves for this detector were calculated by the simulation, and the results are shown in Fig. 11. This detection curve shows that the 8-dB loss in target sensitivity (Fig. 8) has been reduced to about 0.5 dB. However the false rate on clutter extending over four range cells ($N_e = 3$) is about 4%. If there are many patches of clutter which have a range extent of four cells, the reduction of 0.82 will have to be raised. This determination will be made after the detector is connected to the radar. This is possible because the variables k , T , and T_1 are set via switches.

SPS-39 (Lower-Beam)

Since the lower beam of the SPS-39 will encounter clutter, it is necessary to use a CFAR detector. For this reason, two pulses have been transmitted in the lower beam for every pulse in the upper beam. Consequently, as the beam sweeps past the target, 15 hits are obtained. With this number of hits the detector designed for the SPS-12 can be also used for the lower beam of the SPS-39. The only changes required are changes of the feedback values k_1 and k_2 in the integrator and of the values μ , k , T , and T_1 in the second threshold. The values of these parameters for both radars are summarized in Table 4. The numbers for the SPS-39 can also be used for the long-range mode of the SPS-12, with the pulse width increased to 4 μ s and the pulse repetition rate is reduced to 300 pps. The only problem is that with the 4- μ s pulses the reference cells extend over 5 n.mi. and the assumption of homogeneity is less likely to hold.

The detection results of the 15-pulse detector were simulated, and the results are shown in Fig. 12. Comparing the $N_e = 0$ results with the linear detector, one notices that the sensitivity loss is greater for the cases with $M = 15$ pulses. This is to be expected,

* $k = \sqrt{2/\pi}/4.75(0.82)$, where 4.75 is the number of standard deviations of a Gaussian random variable which will yield $P_{fa} = 10^{-6}$.

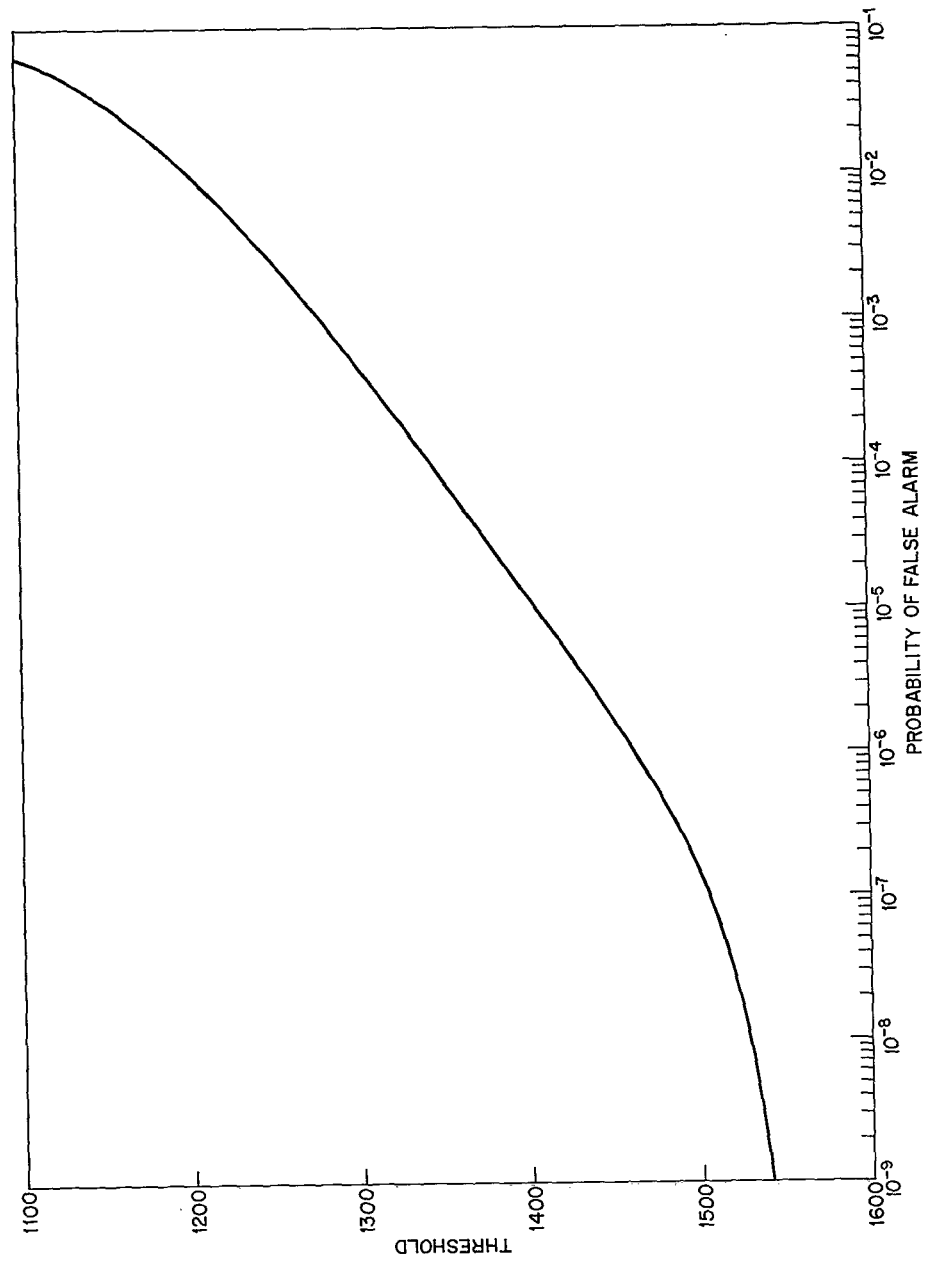


Fig. 10—Probability of false alarm for a given threshold for NRL's generalized sign test when there are $M = 30$ pulses in the beamwidth

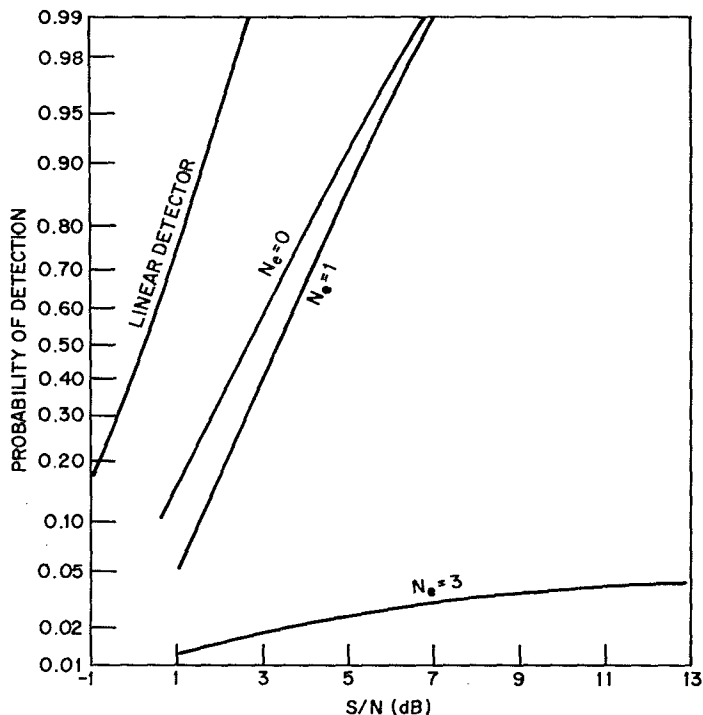


Fig. 11—Probability of detection versus S/N for NRL's generalized sign test with adaptive thresholding ($M = 30$ pulses and $P_{fa} = 10^{-6}$). The linear detector is shown for comparison, and N_e is the number of extraneous targets in the reference cells

Table 4
Parameter Values for the SPS-12 and the Lower Beam of the SPS-39

Radar	k_1 (binary)	k_2 (binary)	k	μ	T	T_1
SPS-12	1.111	0.11110001	0.205	960	1200	102.5
SPS-39	1.11	0.111001	0.185	240	328	31.1

since it is well known [5] that the sensitivity loss associated with nonparametric detectors increases rapidly as the number of pulses decreases. The loss associated with an extraneous target is rather large. This is because of the small number of pulses used and the fact that the estimate of the standard deviation was reduced by only 0.91^* . This factor yields a lower P_{fa} than is yielded for the case $M = 30$ as can be seen by the fact that $P_D < 0.01$ for $N_e = 3$ and $M = 15$ whereas $P_D \approx 0.04$ for $N_e = 3$ and $M = 30$. The optimum value for this factor will be found after data have been collected and analyzed.

*This number was based on the facts that $E|Z - \mu| = 31.59$, $E|Z - (15/14)\mu| = 32.31$, and $E|Z - (15/13)\mu| = 38.65$.

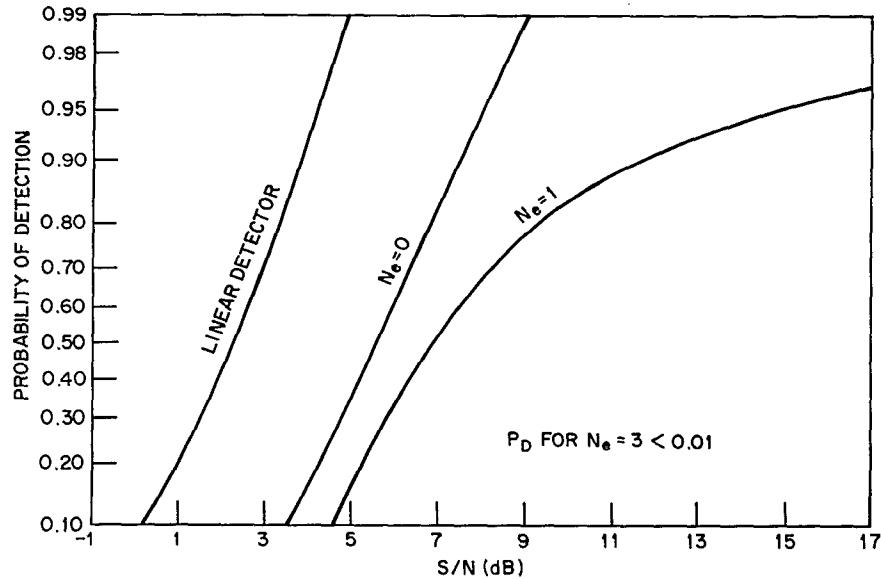


Fig. 12—Probability of detection versus S/N for NRL's generalized sign test with adaptive thresholding ($M = 15$ pulses and $P_{fa} = 10^{-6}$). The linear detector is shown for comparison, and N_e is the number of extraneous targets in the reference cells

SPS-39 (Upper Beam)

The number of hits in the upper beam of the SPS-39 is only eight pulses; consequently it would be expected that the target sensitivity loss for certain nonparametric detectors would be large. The nonparametric detector designed for the SPS-12 and SPS-39 (lower beam) was used for the upper beam, and an 8-dB sensitivity loss was noted. Thus this detector will not be used. Rather two other detectors, a rank detector and a log-Rayleigh detector, will be considered and compared.

Rank Detector

The block diagram of the rank detector is shown in Fig. 13. The test sample is compared to its 16 neighbors, and if the rank of the test sample is greater than k , a 1 is declared. The last eight pulses are saved in shift registers, and their output is summed. If the sum is greater than N , a target is declared. The APL report [2] indicates that if 16 reference cells are used, the optimum value of K is 13 or 14. The P_{fa} rates that can be obtained with various values of K and N are the binomial probabilities shown in Table 5. As the initial values, we will use $K = 14$ and $N = 6$, yielding $P_{fa} = 2.2 \times 10^{-6}$.

Log-Rayleigh Detector

The block diagram of the log-Rayleigh detector is shown in Fig. 14. If the input noise is Rayleigh, the output of the logarithmic detector has a constant standard deviation, independent of the input noise power. Thus only the mean value needs to be

TRUNK, CANTRELL AND QUEEN

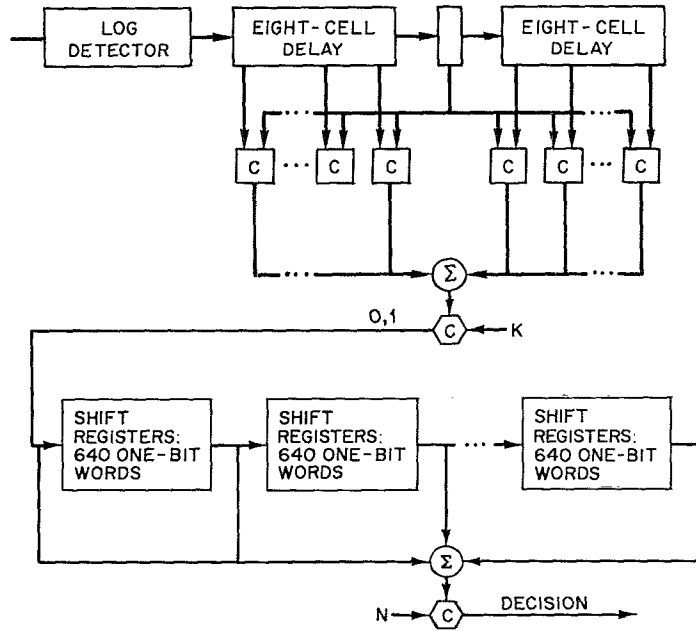


Fig. 13—Nonparametric rank detector with a moving-window integrator

Table 5—Obtainable Values of P_{fa} for the Rank Detector

K	N	P_{fa}
13	5	6.1×10^{-4}
	6	3.6×10^{-5}
	7	9.4×10^{-7}
14	5	6.0×10^{-5}
	6	2.2×10^{-6}
	7	3.6×10^{-8}

estimated. Consequently the first threshold is found by adding a constant K to the average of the reference cells. If the test cell is greater than the first threshold, a 1 is declared; if not, a 0 is declared. Again, the last eight pulses are saved, and their output is summed. If the sum is greater than N , a target is declared. With this detector any false-alarm rate can be achieved. The false-alarm rate of the first threshold can be set to any value by adjusting the parameter K in the following manner: Let x be the input and y be the output of the logarithmic detector. Then

$$1 - P_{fa} = \int_0^T x e^{-x^2/2\sigma^2} / \sigma^2 dx. \quad (17)$$

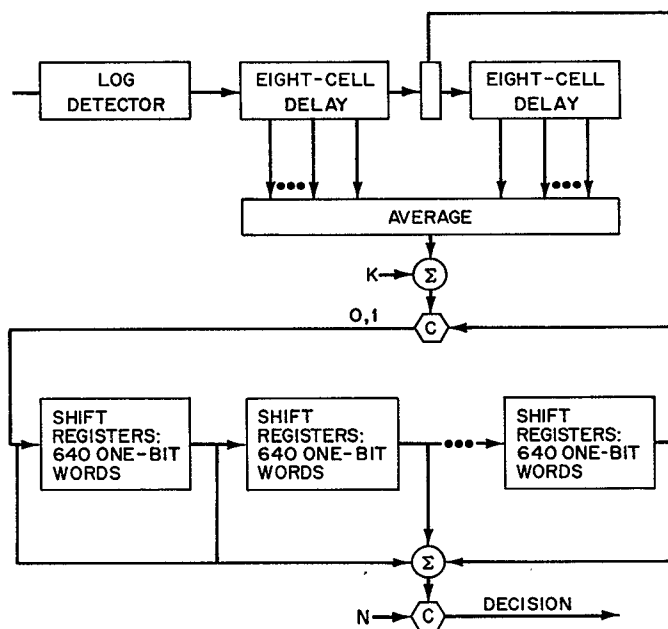


Fig. 14—Log-Rayleigh detector with a moving-window integrator

Solving for T , one obtains

$$T = \sigma \sqrt{-2 \ln P_{fa}}. \quad (18)$$

The threshold T' for the log-Rayleigh detector is found by

$$p(x > T) = P_{fa} \quad (19)$$

and

$$p(y = \ln x > T' = \ln T) = P_{fa}, \quad (20)$$

since \ln is a monotonic function. Thus

$$T' = \ln \sigma + 0.5 \ln (-2 \ln P_{fa}). \quad (21)$$

Noting that the mean for the log-Rayleigh density is [3]

$$\mu_y = \ln \sigma + \frac{\ln 2 - 0.5772157}{2} \quad (22)$$

and that from Fig. 14

$$T' = \hat{\mu}_y + K, \quad (23)$$

one finds that the value of K , which determines P_{fa} , is

$$K = 0.5 \ln(-2 \ln P_{fa}) + \frac{0.5772157 - \ln 2}{2}. \quad (24)$$

Thus, by using Eq. (24), any false-alarm rate can be obtained at the first threshold.

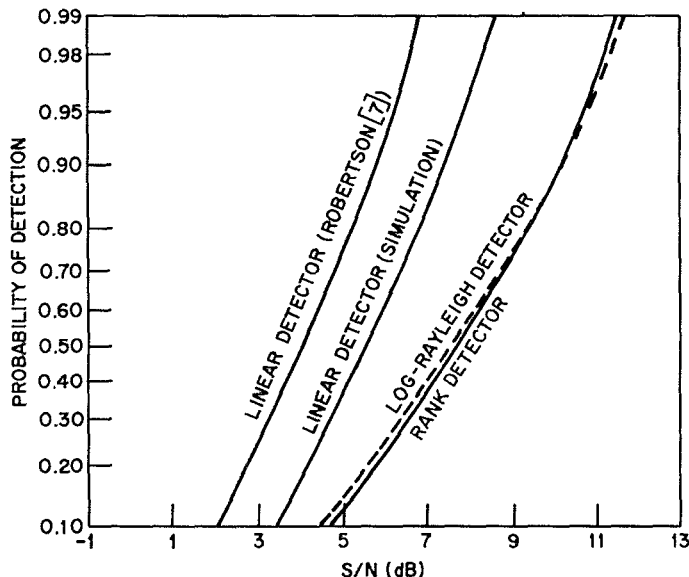


Fig. 15—Probability of detection versus S/N for the linear detector, the rank detector, and the log-Rayleigh detector ($M =$ eight pulses and $P_{fa} = 2.2 \times 10^{-6}$)

Comparison

The detection curves for $P_{fa} = 2.2 \times 10^{-6}$ were found by simulation, and the results appear in Fig. 15. The difference between the simulated and calculated linear-detection curves is the 1.6-dB scanning loss. The differences between the linear detector and the rank and log-Rayleigh detectors is that the noise power was assumed known for the linear detector. Surprisingly there is little difference between the log-Rayleigh and rank detectors. One would have expected the log-Rayleigh detector to be better, since one has correctly assumed that the input noise was Rayleigh. Consequently, since the rank detector is nonparametric and yields CFAR for non-Rayleigh noise, the rank detector will be used for the upper beam.

However, since the integrator and second threshold are identical for both detectors and since the first threshold of the log-Rayleigh detector will be used in the scanning beam of the SPS-39 (next subsection), the log-Rayleigh detector will also be tested on the upper beam.

SPS-39 (Scanning Beam)

At a command from the computer the SPS-39 will stop its search pattern and initiate its normal elevation scan mode [11]. In this mode, only one hit is obtained on the target at many elevation angles. Consequently a simple detector must be used. The detector used is shown in Fig. 16. The only difference between this detector and the first threshold of the log-Rayleigh detector is that the threshold K for the scan mode is set high in order to obtain a low P_{fa} .

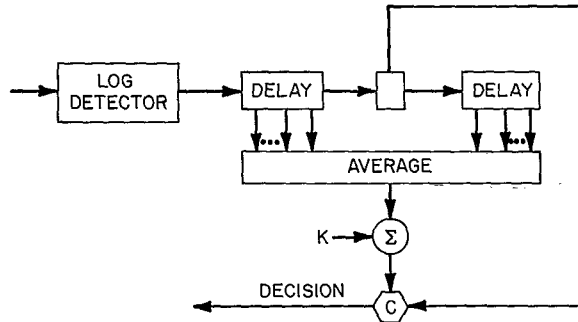


Fig. 16—Log-Rayleigh detector for the scanning mode

The output of this detector will be gated so that only detections between the ranges R_1 and R_2 will be sent to the computer. Initially these ranges will correspond to the leading and trailing edge of the correlation region for the target of interest. Detections are made in this limited region because it is believed that the scanning mode will produce many false alarms. After the equipment is operating, this conjecture can be tested by expanding the acceptance region $[R_1, R_2]$. The region can probably be expanded at high elevations, where no clutter is present. However the acceptance region probably will remain small in the lower elevations which contain clutter.

AZIMUTHAL ESTIMATES

Two azimuthal estimates, threshold crossing and maximum value, were considered for the two-pole integrator [4]. To define the estimates, let the first target detection (FTD) be defined as the smallest i such that $Z_2(i)$ is greater than both detection thresholds and let the last target detection (LTD) be defined as the largest i so that $Z_2(i)$ is greater than both thresholds. The azimuth position of a target can be estimated using a threshold-crossing procedure defined by

$$\hat{\theta} = \frac{1}{2} (\text{FTD} + \text{LTD}) \Delta\theta, \tag{25}$$

where $\Delta\theta$ is the angular scanning increment between successive pulses. The maximum estimate is

$$\hat{\theta} = \Delta\theta (\text{MP}), \tag{26}$$

where MP is the subscript of the largest integrated output; that is, $Z_2(\text{MP}) \geq Z_2(i)$ for all i .

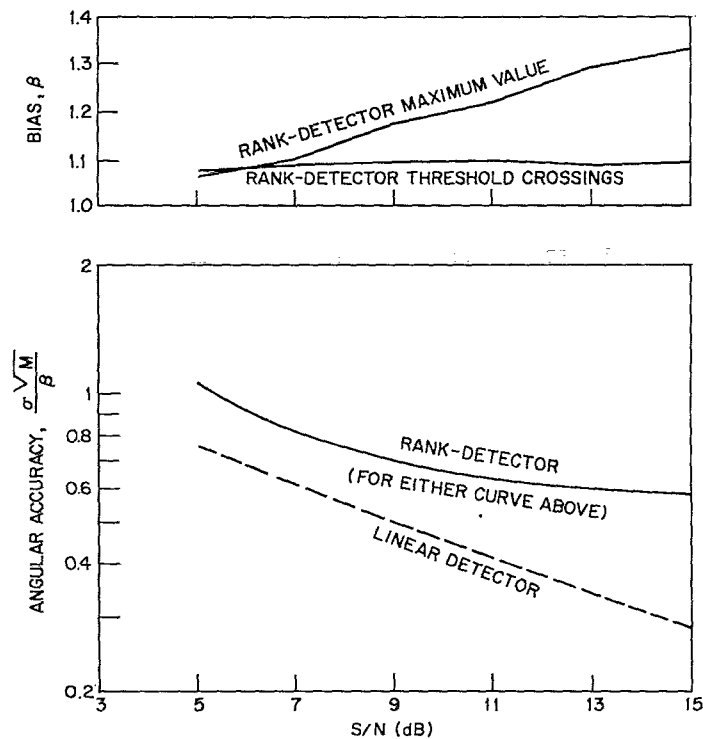


Fig. 17—Comparison of angular estimates, with σ being the standard deviation of the estimation error and M being the number of pulses within the 3-dB beamwidth, which is 2β .

Since the previous study [4] did not include the ranking procedure and the adaptive second threshold, the simulation was repeated, and the results are shown in Fig. 17, where the standard deviation σ of the estimate, the beamwidth 2β , the number of pulses N in the beamwidth, and the S/N per pulse are related by the estimation curve. The standard deviations of the two estimates are the same; consequently only one angular-accuracy curve is plotted for each detector. Comparing the linear and rank detectors, one notices that the linear detector yields much more accurate estimates, especially at higher S/N . From comparison of the two estimates for the rank detector, the threshold-crossing procedure will be used, since its bias value is independent of S/N whereas the bias value of the maximum estimator increases with the S/N .

The implementation of the threshold-crossing estimator is shown in Fig. 18. Radar detections (1 a target or 0 no target) are first gated. If a target has been detected in the preceding range cell on the i th pulse or the following range cell on the $(i - 1)$ th pulse, the detection of a target is inhibited. This logic eliminates a target being detected in adjacent range cells. The gated input on the i th pulse is then compared, with an exclusive or, to the $(i - 1)$ th pulse. Two AND circuits are used to identify the initial detection, a 1, 0 condition, and the final detection, a 0, 1 condition. At the FTD the radar

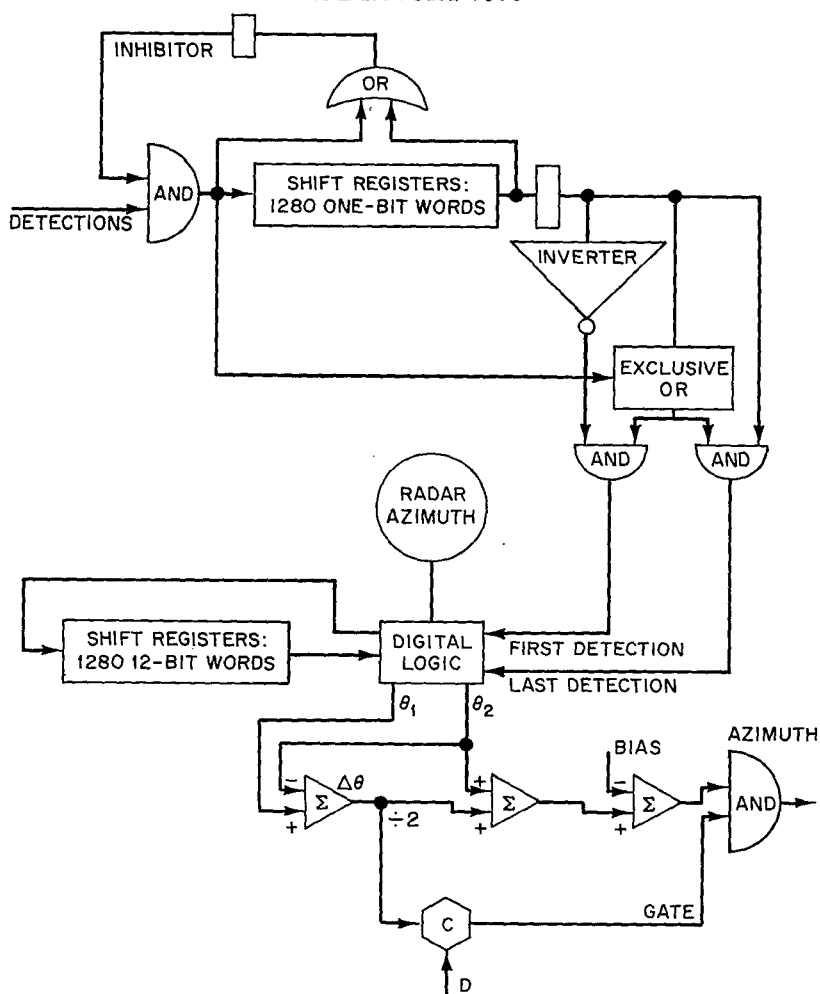


Fig. 18—Circuit which estimates angular position and inhibits certain detections

azimuth is read into a shift register. This value circulates in the shift register until the LTD. At this time both azimuth positions are averaged and the bias value is subtracted to yield the azimuth estimate.* If the difference between the FTD and LTD is greater than D , the detection is assumed to be due to clutter and the output is inhibited. This estimator will be used with all the detectors.

In addition to estimating the azimuth, we are considering modifying this circuit to resolve closely spaced targets. The method used will be based on the idea [12] that a relationship exists between the extent of the threshold crossing and the maximum value. The circuitry will work in the following manner: The extent of the threshold crossing ($\theta_1 - \theta_2$) and the maximum value $\{ \max_i [Z_2(i)] \}$ will be found. Using a read-only memory, a critical value Z will be found for the measured extent. If the maximum value

*The subtractions in Fig. 18 are performed by using one's complement addition. The correct result is always obtained if the result of the addition is never complemented.

is less than Z , two targets are declared. The resolution circuit is not being built because the analysis has not been completed.

SUMMARY

The basic system concept of integrating the SPS-12 2D radar and the SPS-39 3D radar has been described. The SPS-12 and SPS-39 radars are both used for surveillance. The SPS-12 operates in its normal mode, and the SPS-39 operates in a modified mode which attempts to fill in the multipath nulls associated with the SPS-12. Automatic target-detection systems are associated with each radar. These systems not only detect targets but also estimate the target's azimuthal position and inhibit detections in neighboring range cells. The detections are transmitted to the tracking computer and are then displayed on a TV screen. The computer accepts detections from both radars and integrates them into a single track file. The radar operator interacts with the system via the display. The most important operator function is a request for height on selected targets. When a height demand is received, the tracking computer calculates the next update time for the SPS-39 and at this time sends a message to the SPS-39 to stop its search pattern and perform an elevation scan pattern to determine the height of the target.

While the system concept is probably the most important idea in the report, the bulk of the report is concerned with a description of the operation and performance of the automatic target-detection systems. The types of automatic detectors that can be implemented are many and varied. At NRL the judgment has been made that the most important property of the detector is the ability to maintain a constant false-alarm rate (CFAR). This is because an excessive number of false alarms will cause the system (computer) to be overloaded. Consequently a 2-dB target sensitivity loss has been taken in order to maintain a CFAR in a variety of environments. The SPS-12 detector is a modification of the generalized sign nonparametric processor with adaptive thresholding suggested by APL. The detector ranks a sample with its neighboring samples and integrates the ranks with a two-pole filter. The target is declared when the integrated output exceeds two thresholds. The first threshold is fixed and yields a $P_{fa} = 10^{-6}$ when the noise samples are independent and identically distributed. The second threshold is adaptive and maintains a CFAR when the integrated samples are correlated. The device uses the mean deviate estimate, after extraneous targets in the reference cells have been censored, to estimate the standard deviate of the correlated samples. Using Monte Carlo techniques, probability of detection curves and angular accuracy curves have been generated. The detectors for the SPS-39, the rank detector, and the log-Rayleigh detector have also been analyzed, and detection curves are presented.

REFERENCES

1. L.V. Blake, "Machine Plotting of Radio/Radar Vertical-Plane Coverage Diagrams," NRL Report 7098, June 25, 1970.
2. B.H. Cantrell, "Behavior of $\alpha - \beta$ Tracker for Maneuvering Targets Under Noise, False Target, and Fade Conditions," NRL Report 7434, August 17, 1972.
3. Johns Hopkins University, Applied Physics Laboratory, "ARTS Enhancement Support Program Multisensor System Study," MSO-F-141, June 22, 1972.

4. B.H. Cantrell and G.V. Trunk, "Angular Accuracy of a Scanning Radar Employing a 2-Pole Filter," *IEEE Trans., Aerospace and Electronic Systems*, AES-9(No. 5), 649-653 (Sept. 1973).
5. V.G. Hansen and B.A. Olsen, "Nonparametric Radar Extraction Using a Generalized Sign Test," *IEEE Trans., Aerospace and Electronic Systems*, AES-7(No. 5), 942-950 (Sept. 1971).
6. R. Hooke and T. Jeeves, "Direct Search Solution of Numerical and Statistical Problems," *J. Assoc. Comp. Mach.* 8, 212 (1961).
7. G.H. Robertson, "Operating Characteristics for a Linear Detector of CW Signals in Narrow-Band Gaussian Noise," *Bell Sys. Tech. J.* 46, 755-774 (Apr. 1967).
8. L.V. Blake, "The Effective Number of Pulses per Beamwidth for a Scanning Radar," *Proc. IRE* 41, 770-774 (June 1953).
9. H. Urkowitz and R.P. Perry, "A CFAR Technique Insensitive to Nearby Targets," RCA System Technology Memo STM-11011, May 18, 1973.
10. F.S. Hillier and G.J. Lieberman, *Introduction to Operations Research*, San Francisco, Holden-Day, 1967, pp. 457-459.
11. "Technical Manual for Radar Set AN/SPS-39A," Vol. 2, Navships 0967-311-2020 (Confidential), Aug. 2, 1971.
12. J.H. Hughen, "Angular Resolution of Two Targets in a Pulsed Search Radar," NRL Report 7551, Mar. 30, 1973.

Appendix A
MONTE CARLO SIMULATION

The detection performance and angular accuracy of the various detectors is determined by a Monte Carlo simulation. To be specific, the generalized sign nonparametric processor with adaptive thresholding will be discussed. This simulation involves 32 consecutive range cells, with the test cell (the cell that contains the target) being the 17th cell. Initially the integrated output of the center cells, which are used to calculate the adaptive threshold, are set to the average noise level:

$$Z_{-1j} = Z_{0j} = 960, \quad j = 9, \dots, 25.$$

The generation of the pulse-to-pulse radar returns starts at approximately the null of the antenna beam. Specifically, the position of the first pulse was randomized so that the angle between the maximum signal return and the center of the antenna beam was a random variable that was uniformly distributed between $-\Delta\theta/2$ and $+\Delta\theta/2$, where $\Delta\theta$ is the angle moved by the radar beam between successive pulses. The i th received pulse in the j th range cell which contains Rayleigh noise is generated by

$$x_{ij} = \sqrt{-2 \ln U_{ij}},$$

where U_{ij} is a random variable uniformly distributed between 0 and 1. The signal return is generated by

$$x_{ij} = \sqrt{(AG_i^2 + a_{ij})^2 + b_{ij}^2},$$

where G_i is the antenna gain, a_{ij} and b_{ij} are independent zero-mean Gaussian random variables with variance 1, A is the signal strength, and $S/N = 10 \ln (A^2/2)$. The output of the first threshold is

$$r_{ij} = \sum_{k=j-8}^{j+7} u(x_{ij} - x_{ik}), \quad j = 9, \dots, 25,$$

where

$$\begin{aligned} u(x) &= 1, \quad x > 0, \\ &= 0, \quad x \leq 0. \end{aligned}$$

The output of the two-pole integrator for the j th cell is

$$Z_i = k_1 Z_{i-1} - k_2 Z_{i-2} + R_{i-1}.$$

After the integrated outputs Z_{ij} have been generated, an adaptive threshold is calculated using

$$T_1 = 960 + (4.75)(0.82) \sqrt{\frac{\pi}{2}} \frac{1}{N} \sum_{j=9}^{25^*} |Z_{ij} - 960|,$$

where the asterisk indicates that the summation excludes the $j = 17$ term and any other terms in which $Z_{ij} > 1200$ and where N is the number of terms included in the sum. A final threshold T_F is calculated by taking the maximum value of T_1 and a fixed threshold which equals 1460. Finally, a target is declared when

$$Z_{i17} \geq T_F.$$

The angular estimates are made by performing the calculation indicated in Eqs. (25) and (26).

For each S/N , 100 cases were run. Initially S/N was set to 1 dB, and then S/N was incremented by 2-dB steps until 19 dB. The results of the various simulations are shown in Figs. 8, 11, 12, 15, and 17.

Appendix B IMPORTANCE SAMPLING

The straightforward method of determining the required threshold for a given false-alarm rate for the statistic Z_{ij} is to perform a Monte Carlo simulation. Unfortunately for $P_{fa} = 10^{-6}$ over 10^6 repetitions would need to be run and the required computer time would be large, approximately 2 hours for $M = 15$ pulses and 10^6 repetitions.

However an indirect approach that uses importance sampling* can be used. The fundamental principle of the technique of importance sampling is to modify the probabilities that govern the outcome of the basic experiment of the simulation is such a way that the event of interest (the false alarm) occurs more frequently. This distortion is then compensated for by weighting each event by the ratio of the probability that this specific event would have occurred if the true probabilities had been used in the simulation to the probability that this same event would occur with the distorted probabilities. Consequently, by proper choice of the distorted probabilities, the number of repetitions can be reduced greatly.

To illustrate the method, let us generate the distribution function for Z_{ij} for the case $M = 15$ pulses. In the straightforward method, Z_{ij} is initialized to its average value of 240, and 30 random integers R_{ij} are generated having the true probabilities

$$P_T(R_{ij} = \ell) = \frac{1}{16} \quad \ell = 0, \dots, 15.$$

The 30 random integers are integrated using Eq. (6), the result is quantized into an interval, and a probability of $1/M_c$ is associated with this interval. The simulation is repeated M_c times, and a cumulative density (and hence a distribution) results.

In the importance sampling method, Z_{ij} is initialized to its average value of 240, and 30 random numbers are generated having the distorted probabilities

$$P_D(R_{ij} = \ell) = \frac{(\ell + 1)}{136}, \quad \ell = 0, \dots, 15.$$

The random numbers are again integrated, the result is quantized into an interval, and a probability

*F.S. Hillier and G.V. Lieberman, *Introduction to Operations Research*, San Francisco, Holden-Day, 1967, pp. 457-459.

$$\frac{1}{M_c} \prod_{j=1}^{30} \frac{P_T(R_{ij})}{P_D(R_{ij})} = \frac{\left(\frac{1}{16}\right)^{30}}{M_c \prod_{j=1}^{30} P_D(R_{ij})}$$

is associated with the interval. The results for $M_c = 2 \times 10^4$ (2 minutes of computing time) are shown in Fig. B1. Thus a threshold of 408 corresponds to $P_{fa} = 10^{-6}$. The results for the case $M = 30$ pulses are shown in Fig. 10.

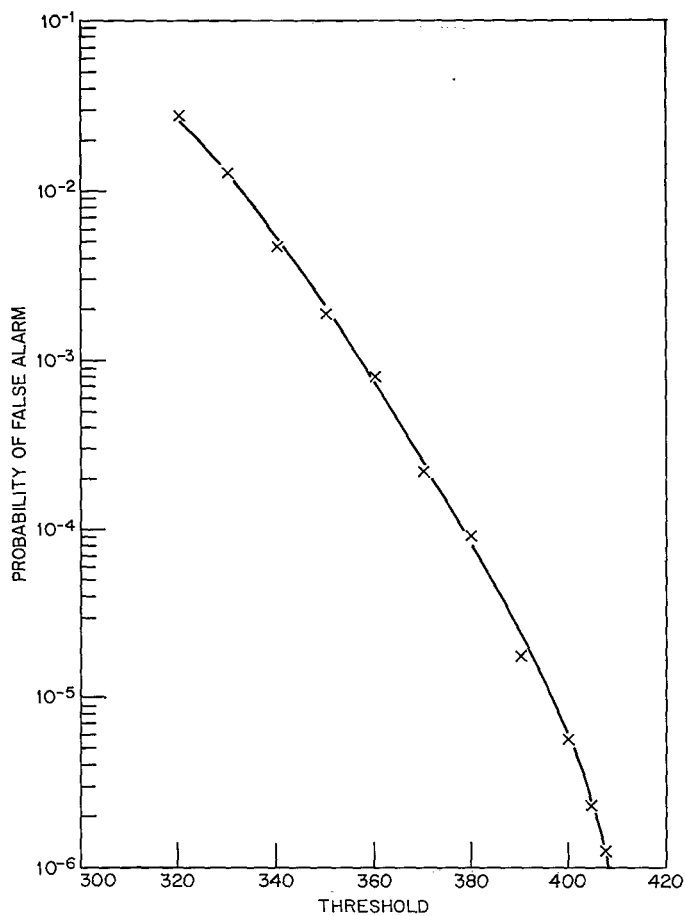


Fig. B1—Probability of false alarm for a given threshold for the NRL generalized sign test when there are $M = 15$ pulses in the beamwidth